friction in the overall drive.

We should note that the fingers in this device are serrated and designed to hold needles. However, they could be made as retractors, microforceps, dissecting scissors, blades, etc.

5.2.2.3 Proximal Portion

The proximal portion of the wrist comprises an actuator package which drives the wrist and fingers, rotation of the instrument shaft about its long axis, axis C, and translation along this axis.

The proximal portion of the wrist unit, 28a, includes the aluminum support brackets 98 and 102, which are connected via two .250 diameter stainless steel guide shafts. A single 4-point-contact bearing (Kaydon KAA10XL0) is housed in bracket 98 to support the instrument shaft, 24. Such bearings support radial, moment and axial loads and can be used in place of two radial bearings. Four ball bushings (Thomson SUPER-4) are mounted in motor bracket, 96, to form a bearing for the translational DOF. The brackets 96, 98, and 102 are line bored to assure parallelism of the shafts so that the ball bushings do not bind. The lengths of the shafts were chosen to allow nine inches of travel. The motors M2-M6 are face mounted to the outside of bracket, 96, which is essentially a rectangular hollow tube. Each motor has a threaded drive capstan which engages one cable as shown in Figure 5-11 and forms a friction drive. Two or three wraps is sufficient to prevent the cable from slipping on the capstans since the ratio of low to high tension sides of the cable increases exponentially with angular contact:

$$\frac{T_1}{T_2} = ke^{\mu\theta}$$

where T_1 is the high tension side, T_2 is the low tension side, μ is the coefficient of friction, θ is the wrap angle, and k is a proportionality constant.

check this!

Threading the pinions prevents the cable from rubbing on itself as it travels over the capstans. Also, the threads are semicircular in cross-section so that the cable deforms minimally as it rolls onto and off of the capstans. This is again to minimize friction generated within the cable itself. We use uncoated 7×19 constructuion .018 diamter stainless steel aircraft cable (SAVA Industries, NJ) in the wrist unit.[2] We find that cable coatings add a substantial amount of friction to cable transmissions

[2] I have recently seen a sample of very nice 19×7 cable manufactured by Baird, also in NJ. This

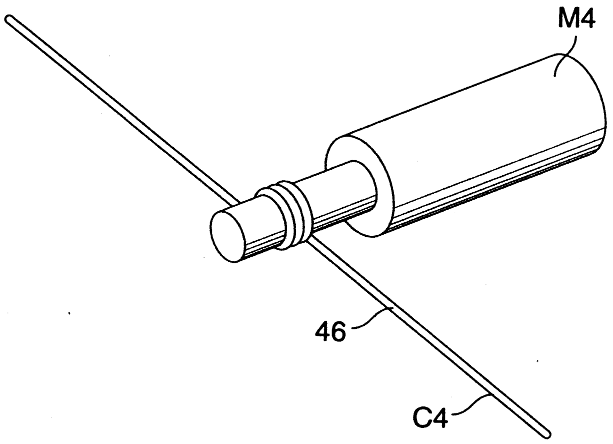

Figure 5-11: Drive layout for single motor and cable.

due to the compression of the coating as it rolls onto pulleys. At the same time, the static sliding friction between the cable and the driving capstans is reduced, which is unsatisfactory for a friction drive system. The motors are Maxon RE025-055-035 brushed d.c. motors with graphite brushes which have zero cogging and very low rotor inertia. The encoders are Hewlett-Packard HEDS-5500 series optical encoders with 1024 lines (4096 counts with quadrature) per revolution mounted on the rear of the motors, which are reliable and inexpensive. Motors M3-M6 actuate the four wrist cables, and motor M2 actuates rotation about the instrument shaft, axis C, as described below.

The cable actuation scheme for rotation about the instrument shaft, axis C, is shown in Figure 5-12. A single cable loop, C5, runs about idler pulleys 83, 84 and 85. Pulley 83 rides in a shaft which is mounted on a fork. This fork is attached via a tensioning mechanism (tensioned using a screw) to bracket 102 to adjust tension in the cable. The driven capstan, 90, is also threaded and fixed directly to the proximal end of the instrument shaft, 24. The pulleys 84 and 85 are fixed via a piece not shown onto the guide shaft, 102. This mechanism is similar functionally to a traditional spline, though in this case, the motor, M2, turns during linear motion of the instrument.

cable was drawn through a mandrel and very round and smooth externally. It also used smaller fiber sizes to improve fatigue strength. At the time of this writing I have not had a chance to test this cable.

5.2.2.4 Cabling Scheme - Simplified Version

Here we describe the $N+1$ cabling scheme used in the wrist described above. The cable layout is shown in Figure 5-12. The fingers 20a and 20b, wrist member 22, and the translation of instrument 12 along axis C are driven by cables C1, C2, C3, and C4. Driving N freedoms with $N+1$ cables is known as an $N+1$ actuation scheme. This represents the minimum number of tension elements needed to actuate N freedoms. (J.K. Salisbury, 1982)

In Figure 5-12, the rotational motion about the instrument shaft, axis C, is omitted in order to more easily show cables C1-C4. Such rotation results only in twisting of the cables C1-C4 between motors M3-M6 and pulleys 70, 72, 74, 76. Due to the length of the instrument shaft, however, the resulting change in length of the cables is slight, and the length of the cables is long, so that the resulting resistance to rotational motion is on the order of bearing friction in joint 26, and substantially less than torque due to brush friction in motor M2. (Discussion of friction values and performance specifications in general may be found in Section 5.5). This twisting of cables C1-C4 does, however, limit rotation of the instrument shaft to $\pm$ 180° at which point the cables will rub on each other creating friction and wear.

As shown in Figure 5-12, cables C1 and C2 form two sides of a continuous cable loop 44. Cable C1 of loop 44 engages a proximal idler pulley 80, the drive shaft of motor M4, intermediate idler pulley 70 and driven capstan 18a. Cable loop 44 returns from driven capstan 18a as cable C2 and engages intermediate idler pulley 76, the drive shaft of motor M5 and proximal idler pulley 80. The cable is fixed under the head of a single #0-80 screw in order to fix it to the capstan. Conventional tin-lead solder can also work if an appropriate flux is used for stainless steel, though this does not allow room for later adjustment without recabling, and application of heat may detemper and weaken the cable.

Continuing with the description, cables C3 and C4 form two sides of a continuous loop of cable 46. Cable C3 of cable loop 46 engages proximal idler pulley 78, the drive shaft of motor M3, intermediate idler pulley 72 and driven capstan 18b. Cable loop 46 returns from driven capstan 18b as cable C4 and engages intermediate idler pulley 74, the drive shaft of motor M6 and proximal idler pulley 78.

The proximal idler pulleys 78 and 80 are tensioned by cables C6 and C7 which are fixed kinematically to the center of proximal idler pulleys 78 and 80. The pulleys in fact ride on shafts held in small forks into which the cables terminate. Each pulley uses a single ball bearing. Cables C6 and C7 form two sides of a single cable 45 which engages proximal idler pulley 82. Pulley 82 rides on a shaft held in a fork. This fork is mounted via a tensioning mechanism to the bracket 102 which allows turning of

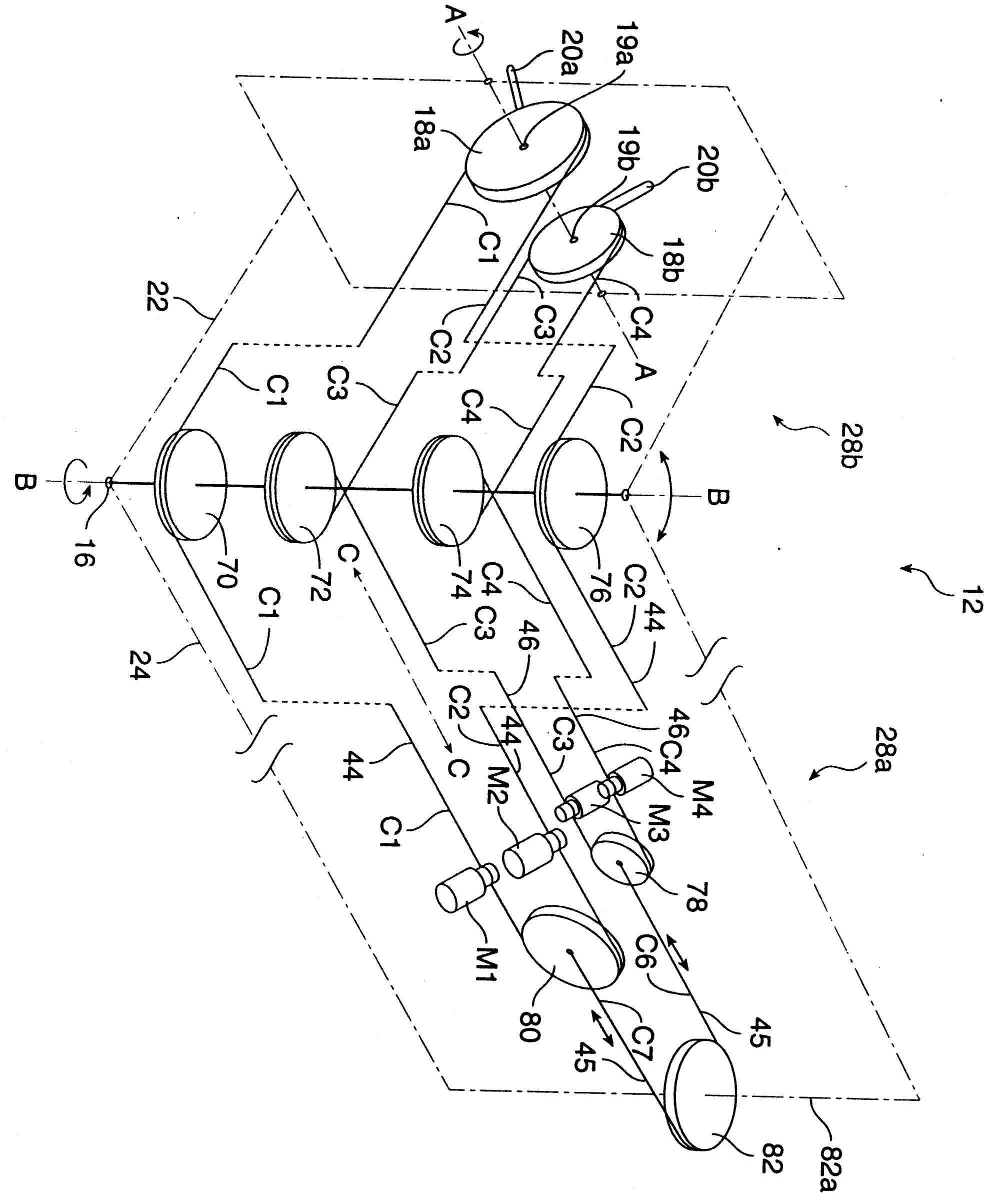

Figure 5-12: $N + 1$ Cable actuation scheme for wrist.

a screw in order to tension the cables. The cables are arranged so that this single tensioning point tensions all cables C1-C7.

The use of proximal idler pulleys 78, 80, and 82 is unusual in $N+1$ cabling schemes. Typically, a seperate motor is used for each of the $N+1$ cables, as suggested in (Burdea and Zhuang, 1991). Using an extra motor has the advantage that the overall pretension in the system is actively adjustable, which is useful when using a relatively high friction transmission such as cable conduits as in the Salisbury Hand. However the disadvantages are that an extra motor is required, and tension is lost when motor power is turned off. This results in an unravelling of cables at the driving capstan where multiple wraps are used to drive the cable. A pretensioned $N+1$ arrangement is much more convenient while maintaining the advantage of minimizing cables which must past through the shaft into the wrist and simplifying the wrist design.

In order for all the cables to align properly with all the pulleys, pulleys 78 and 80 will need to be made different diameters. In addition, the mounting locations of motors M2-M6 on bracket 96 must be selected very carefully to ensure cables C1-C5 align exactly tangentially to the driving capstans on motors M2-M6. Since the cables make several wraps on each driving capstan, and each capstan is threaded accordingly, the cable will walk axially along the capstan as the motor turns. In practice, the axial cable motion is approximately .25 inches over the length of travel so that this does not cause a problem.

The movement of the wrist and fingers is caused by coordinated motion of the motors. If motors M4 and M5 act in opposition, finger 20a will rotate. Similarly if motors M3 and M6 act in opposition, finger 20b will rotate. These seperate rotations acting against each other provide gripping. If motors M3 and M5 act in the same direction, and motors M4 and M5 act in the same direction, but in opposition to M3 and M5, then the wrist will pitch about axis B. Finally, if all motors M3, M4, M5, and M6 act together, the entire wrist unit will translate along axis C. The exact differential transformations for the wrist described below, which is actually used in the Silver Falcon, will be given in section 5.2.3.

5.2.2.5 Cable Scheme - Non-α Version

The cabling scheme described above has the problem that the cables are forced to cross over themselves and form a slight helix as they make complete wraps around the intermediate idler pulleys, 70, 72, 74, and 76. We call this type of wrap an α-wrap[3].

[3] The author first heard this term from Tom Cooper at Intuitive Surgical, Inc. The term was originally used to describe tape drive mechanisms.

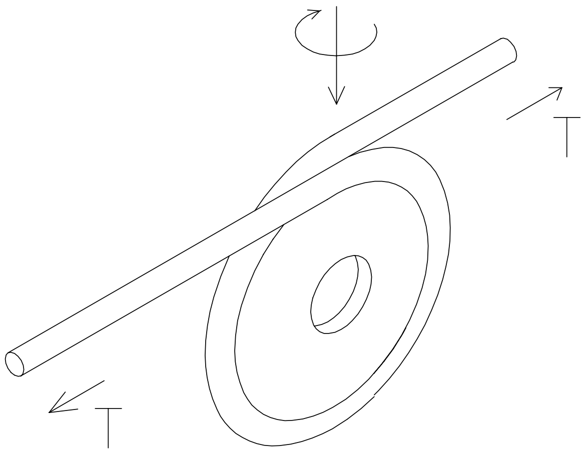

Figure 5-13: The α-wrap causes two problems. (a) the cable rubs on itself, and (b) it causes the pulley to tilt. If T is the tension on the cable, then there is a a torque on the pulley equal to T$\times$d where d is the cable diameter.

The helix causes two problems, see Figure 5-13. First, the cable tends to rub on itself which creates extra friction. Second, a torque is placed on the pulley which causes it to tilt about an axis orthogonal to the pulley shaft. This is because the cable comes onto the pulley approximately one cable diameter to the side of where it comes off of the pulley. Since the single pulley bearings are not designed to handle moments, tilting the pulley forces the pulley to rub on its neighboring pulley for support creating additional friction. Also the bearing itelf is not meant to run tilted creating yet more friction.

As a result, a modified wrist was designed which eliminated α-wraps. A top view of this design is shown in Figure 5-14. The addition of four extra pulleys add complexity and adds friction at the pulley bearings and due to bending of the cables on these pulleys. However, the fact that the pulleys are relieved of tilting moments and do not rub on each other for support more than compensates for the addition.

This represents the wrist implementation on the Silver Falcon. The kinematics relationships change slightly, though the change is straightforward. The relationships given in the next section reflect this change.

5.2.3 Differential Kinematics

Here we give the relationship between motor velocities and joint velocities, and similarly motor torques to joint torques for the wrist unit. These relationship are repre-

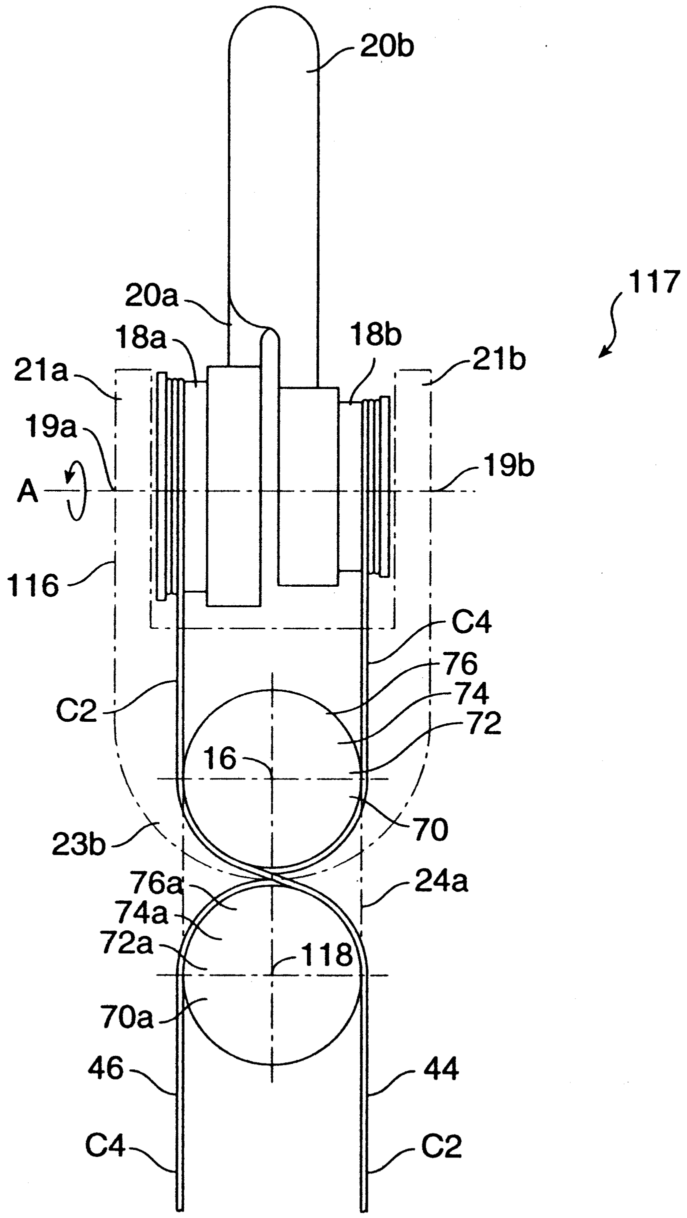

Figure 5-14: $N+1$ Cable actuation scheme for the non-α wrist. This wrist reduces friction by avoiding all α-wraps within the wrist.

sented as linear trasformations as follows:

$$\dot{\mathbf{q}} = J_{motor \rightarrow joint} \dot{\mathbf{m}} \tag{5.6}$$

$$\boldsymbol{\tau}_m = J^T_{motor \rightarrow joint} \boldsymbol{\tau}_j \tag{5.7}$$

where $\dot{\mathbf{m}}$ are motor velocities, $\dot{\mathbf{q}}$ are joint velocities, $\boldsymbol{\tau}_m$ are motor torques, $\boldsymbol{\tau}_j$ are joint torques, and and $J_{motor \rightarrow joint}$ is a constant linear transformation.

We define the joints of the Silver Falcon 0-6 (seven joints total) as shown in Figure 5-2. Definitions of the positive direction of rotation are also given in the figure.

The speed ratios are defined as:

R_{LC}	268.04 rad/meter	Motor to cable velocity ratio
R_{SC}	396.75 rad/meter	Motor to cable velocity ratio
R_P	.00417 meter/rad	Cable velocity to wrist pitch velocity ratio
R_{SF}	1.519 rad/rad	Motor to finger ratio
R_{LF}	1.580 rad/rad	Motor to finger ratio
R_R	5.291 rad/rad	Motor to roll axis ratio

The relationship between motor velocities and joint velocities is:

$$\begin{pmatrix} \dot{q}_2 \\ \dot{q}_3 \\ \dot{q}_4 \\ \dot{q}_5 \\ \dot{q}_6 \end{pmatrix} = \begin{pmatrix} 0 & \frac{1}{4R_{LC}} & \frac{-1}{4R_{SC}} & \frac{-1}{4R_{SC}} & \frac{1}{4R_{LC}} \\ \frac{-1}{R_R} & \frac{-R_{SC}}{4R_R R_{LC}} & \frac{1}{4R_R} & \frac{1}{4R_R} & \frac{-R_{SC}}{4R_R R_{LC}} \\ 0 & \frac{1}{4R_{LC}R_P} & \frac{1}{4R_{SC}R_P} & \frac{1}{4R_{SC}R_P} & \frac{1}{4R_{LC}R_P} \\ 0 & \frac{-1}{2R_{LF}} & \frac{-1}{2R_{SF}} & \frac{1}{2R_{SF}} & \frac{1}{2R_{LF}} \\ 0 & \frac{-1}{4R_{LF}} & \frac{1}{4R_{SF}} & \frac{-1}{4R_{SF}} & \frac{1}{4R_{LF}} \end{pmatrix} \begin{pmatrix} \dot{m}_2 \\ \dot{m}_3 \\ \dot{m}_4 \\ \dot{m}_5 \\ \dot{m}_6 \end{pmatrix} \tag{5.8}$$

where the above matrix is $J_{motor \rightarrow joint}$. The transpose relates joint torques to motor torques:

$$\begin{pmatrix} \tau_{m2} \\ \tau_{m3} \\ \tau_{m4} \\ \tau_{m5} \\ \tau_{m6} \end{pmatrix} = \begin{pmatrix} 0 & \frac{-1}{R_R} & 0 & 0 & 0 \\ \frac{1}{4R_{LC}} & \frac{-R_{SC}}{4R_R R_{LC}} & \frac{1}{4R_{LC}R_P} & \frac{-1}{2R_{LF}} & \frac{-1}{4R_{LF}} \\ \frac{-1}{4R_{SC}} & \frac{1}{4R_R} & \frac{1}{4R_{SC}R_P} & \frac{-1}{2R_{SF}} & \frac{1}{4R_{SF}} \\ \frac{-1}{4R_{SC}} & \frac{1}{4R_R} & \frac{1}{4R_{SC}R_P} & \frac{1}{2R_{SF}} & \frac{-1}{4R_{SF}} \\ \frac{1}{4R_{LC}} & \frac{-R_{SC}}{4R_R R_{LC}} & \frac{1}{4R_{LC}R_P} & \frac{1}{2R_{LF}} & \frac{1}{4R_{LF}} \end{pmatrix} \begin{pmatrix} \tau_{j2} \\ \tau_{j3} \\ \tau_{j4} \\ \tau_{j5} \\ \tau_{j6} \end{pmatrix} \tag{5.9}$$

There are several things to note from the above relationships.[4]

[4]For reference, the Silver Falcon software calls R_P above R_Y. That is this pitch axis is referred to a yaw axis in the software. We have renamed it pitch here for consistency.

- Two motors contribute to the torque applied to each finger. As a result, given the same speed ratios, the gripping force possible with this design is twice that of a more conventional design where a single motor operates each finger, or a single degree of freedom gripper. A caveat is that if torques are being supplied to other joints, the grip force possible is reduced.

  An additional advantage is that finger velocities are an average of two measurements which makes them smoother. From a velocity estimation standpoint, the encoder resolution is doubled.

- Four motors contribute to the translational axis. This is good because this axis must use a portion of the torque available to counterbalance itself actively. It turns out that in order to do so, each motor uses less than 10% of its available torque. The velocity estimate is the average of four encoder readings so resolution is quadrupled.

- Four motors also contribute to joint 4 torques (pitch) which is good because the tips of the fingers are twice as far away from this axis than they are from the finger axes. Again the same advantage with velocity estimation is achieved.

5.3 Master

Our master manipulator is the Phantom haptic interface described in (Massie and Salisbury, 1994), and shown in Figure 5-15. A schematic showing the Phantom kinematics is shown in Figure 5-16. The cartesian axes in the figure are aligned with those shown in Figure 5-2 during use of the system. The system is shown in its zero position. The system is essentially a three degree of freedom manipulator which is approximately counterbalanced using the weight of its own motors. The standard Phantom uses a passive three axis gimbal at the end of the actuated three axis arm. We replaced the gimbal with a version which uses panel mount optical encoders (Bourns) to measure the gimbal positions. A seventh degree of freedom was added to the last link of the gimbal to control gripping motion of the slave manipulator. The master gripper uses a spring return so that the user can operate them somewhat like a pair of tweezers. Figure 5-17 shows how the user holds the master.

The link lengths are given by:

$$\begin{aligned} l_1 &= 0.143 \text{ m} \\ l_2 &= 0.178 \text{ m} \end{aligned}$$

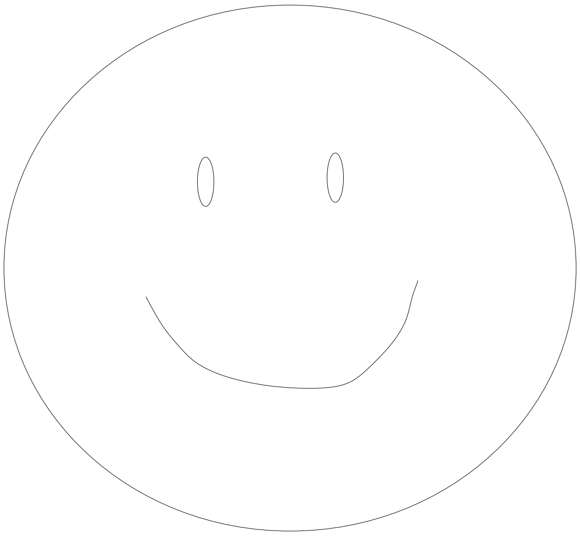

Figure 5-15: The Phantom Haptic interface modified for use as master manipulator for the Silver Falcon.

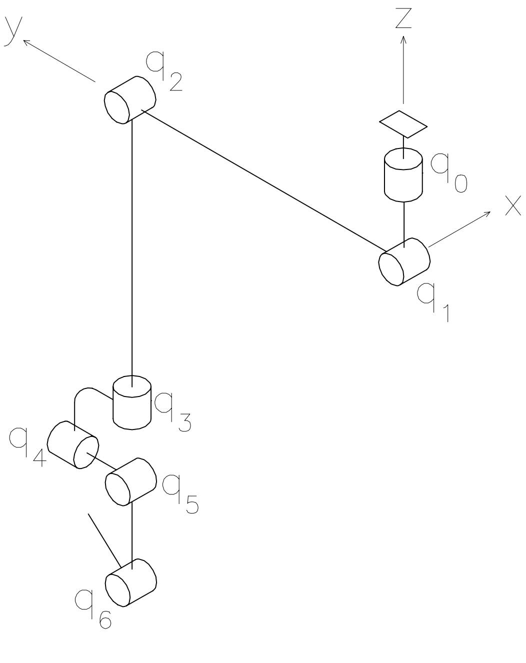

Figure 5-16: The Phantom Haptic interface kinematics. The system is shown in its zero position.

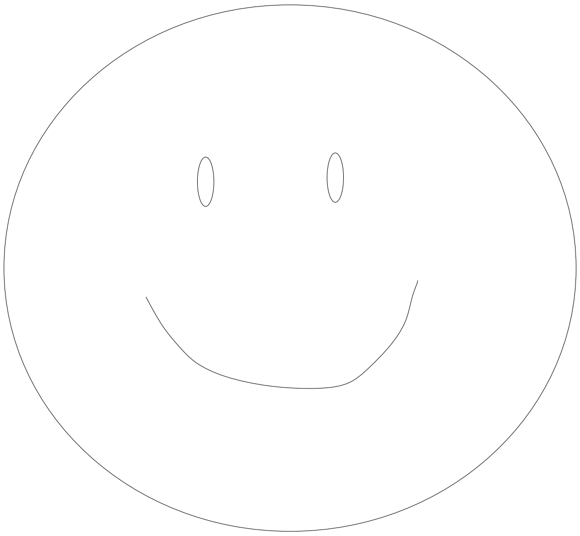

Figure 5-17: A passive gripper added to the end of the Phantom Haptic interface to control gripping on the Silver Falcon.

and the speed ratios are given by:

$$R_0 = 9.970$$
$$R_1 = 9.936$$
$$R_2 = 9.936$$

Each motor is capable of producing 29.61 mNm of maximum continuous torque. At 2 times max rated continuous torque (which is typically how we run the system), we can achieve maximum endpoint force values of:

$$f_{MX} = 4.1 \text{ N}$$
$$f_{MY} = 4.1 \text{ N}$$
$$f_{MZ} = 3.3 \text{ N}$$

Each encoder is a Hewlett-Packard optical encoder with 2000 counts/revolution (after quadrature). This gives an endpoint measurement resolution of:

$$r_x = 4.51 \times 10^{-5} \text{ m}(1.77 \times 10^{-3} \text{ in})$$
$$r_y = 5.63 \times 10^{-5} \text{ m}(2.22 \times 10^{-3} \text{ in})$$
$$r_z = 4.52 \times 10^{-5} \text{ m}(1.78 \times 10^{-3} \text{ in})$$

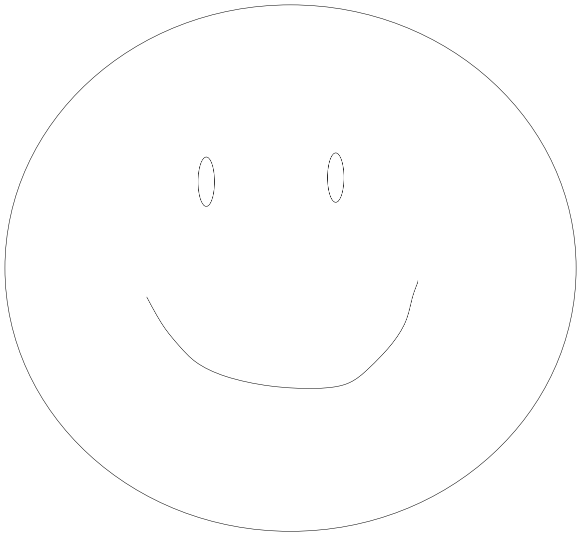

Figure 5-18: Actuated gripper “left-hand” master interface. This allows force reflection of the gripper to be felt by the user while still using the Phantom haptic interface as a master manipulator.

Because this passive gripper does not allow the user to feel forces, we developed a second *actuated gripper* interface to control gripping. Because the master cannot carry the weight of such an actuated gripper, it was mounted on a table stand so as to be used with the user’s left hand, while the Phantom is used with the right hand. The actuated gripper consists of a pair of standard needle holder handles attached to a single rotary axis. One handle is fixed to ground, while the other is attached via a cable transmission to a brushed d.c. electric motor (Maxon RE025-055-035, graphite brushes). Figure 5-18 is a photo of the system.

5.4 Controller

The basis for the controllers implemented on this system was described in Chapter 3, Macro Micro Control. The implementation on the full 7 degree of freedom Silver Falcon was done by Dr. Günter Niemeyer of the MIT AI Lab, and will be described in a forthcoming publication.